Contributions of Engineered Surface Salt Bridges to the Stability of T4 Lysozyme Determined by Directed Mutagenesis[†,‡]

Sun Dao-pin,[§] Uwe Sauer, Hale Nicholson, and Brian W. Matthews*

Institute of Molecular Biology, Howard Hughes Medical Institute, and Department of Physics, University of Oregon, Eugene, Oregon 97403

Received January 24, 1991; Revised Manuscript Received April 25, 1991

ABSTRACT: Six designed mutants of T4 lysozyme were created in an attempt to create putative salt bridges on the surface of the protein. The first three of the mutants, T115E (Thr 115 to Glu), Q123E, and N144E, were designed to introduce a new charged side chain close to one or more existing charged groups of the opposite sign on the surface of the protein. In each of these cases the putative electrostatic interactions introduced by the mutation include possible salt bridges between residues within consecutive turns of an α-helix. Effects of the mutations ranged from no change in stability to a 1.5 °C (0.5 kcal/mol) increase in melting temperature. In two cases, secondary (double) mutants were constructed as controls in which the charge partner was removed from the primary mutant structure. These control proteins indicate that the contributions to stability from each of the engineered salt bridges is very small (about 0.1–0.25 kcal/mol in 0.15 M KCl). The structures of the three primary mutants were determined by X-ray crystallography and shown to be essentially the same as the wild-type structure except at the site of the mutation. Although the introduced charges in the T115E and Q123E structures are within 3–5 Å of their intended partner, the introduced side chains and their intended partners were observed to be quite mobile. It has been shown that the salt bridge between His 31 and Asp 70 in T4 lysozyme stabilizes the protein by 3–5 kcal/mol [Anderson, D. E., Becktel, W. J., & Dahlquist, F. W. (1990) *Biochemistry 29*, 2403–2408]. To test the effectiveness of His···Asp interactions in general, three additional double mutants, K60H/L13D, K83H/A112D, and S90H/Q122D, were created in order to introduce histidine–aspartate charge pairs on the surface of the protein. Each of these mutants destabilizes the protein by 1–3 kcal/mol in 0.15 M KCl at pH values from 2 to 6.5. The X-ray crystallographic structure of the mutant K83H/A112D has been determined and shows that there are backbone conformational changes of 0.3–0.6 Å extending over several residues. The introduction of the histidine and aspartate presumably introduces strain into the folded protein that destabilizes this variant. It is concluded that pairs of oppositely charged residues that are on the surface of a protein and have freedom to adopt different conformations do not tend to come together to form structurally localized salt bridges. Rather, such residues tend to remain mobile, interact weakly if at all, and do not contribute significantly to protein stability. It is argued that the entropic cost of localizing a pair of solvent-exposed charged groups on the surface of a protein largely offsets the interaction energy expected from the formation of a defined salt bridge. There are examples of strong salt bridges in proteins, but such interactions require that the folding of the protein provides the requisite driving energy to hold the interacting partners in the correct rigid alignment.

It has long been known that salt bridges can play an important role in protein structure and function (e.g. see Perutz, 1978). Some salt bridges, including the His 31 to Asp 70 salt bridge in T4 lysozyme (Anderson et al., 1990), the α-ammonium ion of Ile 16 to Asp 194 salt bridge in α-chymotrypsin (Fersht, 1972), and the amino terminus to carboxyl terminus salt bridge in BPTI (Brown et al., 1978), have been shown to provide stabilization energies ranging from 1 to 5 kcal/mol. Charged groups in proteins are not distributed uniformly but tend to be surrounded by groups of the opposite charge, suggesting that electrostatic interactions between such groups contribute to protein stability (Wada & Nakamura, 1981; Barlow & Thornton, 1983). On the other hand, recent studies have suggested that some electrostatic interactions contribute little to protein stability (Pace et al., 1990; Serrano et al., 1990; Erwin et al., 1990; Dao-pin et al., 1991b).

With T4 lysozyme as a model, six charge pairs have been designed and constructed to examine the energetics associated with these salt bridge interactions. The variants consist of three single mutants, T115E (Thr 115 to Glu), Q123E, and N144E, designed to introduce glutamates close to existing lysines or arginines, as well as three double mutants, K60H/L13D, K83H/A112D, and S90H/Q122D, designed to introduce His···Asp ion pairs. Additional control mutants were also constructed to determine whether any changes in stability were due to electrostatic or other effects. The thermostabilities of the mutants were measured by circular dichroism monitored reversible thermal denaturation. The structures of four of the primary mutants have been determined by high-resolution X-ray crystallography, and the pK_a values of His 60, His 83, and His 90 in the three histidine-containing mutants were measured by NMR. The results suggest that the electrostatic interaction energy between pairs of mobile, solvent-exposed,

[†]This work was supported in part by grants from the NIH (GM21967) and from the Lucille P. Markey Charitable Trust.

* To whom correspondence should be addressed.

[‡]Coordinates of the refined mutant structures have been deposited in the Brookhaven Protein Data Bank (code numbers 1L37, 1L38, 1L39, 1L40, and 1L41).

[§]Present address: Laboratory of Molecular Biology, National Institute of Diabetes, Digestive and Kidney Diseases, National Institutes of Health, Bethesda, MD 20892.

0006-2960/91/0430-7142$02.50/0

Table I: Putative Salt Bridges[a]

mutant name	putative salt bridge	side-chain solvent accessibility (%) (+)	(−)	activity (%)
T115E	Lys 83···Glu 115	73	73	370
Q123E	Arg 125···Glu 123	54	55	280
	Arg 119···Glu 123		55	
N144E	Lys 147···Glu 144	52	73	115
S90H/Q122D	His90···Asp 122	40	60	100
K83H/A112D	His 83···Asp 112	73	14	110
K60H/L13D	His 60···Asp 13	59	28	115

[a] The fractional surface area of the respective side-chains of the positive (+) and negative (−) partners exposed to solvent were estimated from model-built coordinates by using the algorithm of Lee and Richards (1971). Activities were determined with the assay of Tsugita et al. (1968) and have an estimated error of ±20%. Each value is the average of at least two determinations.

charged residues on the surfaces of proteins is weak. Charged groups that are held rigidly in close apposition may, however, interact strongly.

Materials and Methods

Choice of the Mutations. Two different types of mutations were considered. The first was designed to examine interactions on the surface of the protein between the common basic (Lys, Arg) and acidic (Asp, Glu) side chains. T4 lysozyme is a basic protein with a net formal positive charge of 9 units at neutral pH. Most of the acidic groups in the wild-type structure are close to basic groups or to the amino termini of α-helices. Therefore a series of mutants (T115E, Q123E, and N144E) was designed to introduce either an aspartate or a glutamate close to positively charged residues. The second type of mutation was intended to explore interaction with histidine. There is only a single histidine (His 31 in wild-type lysozyme), and it forms a very strong (3–5 kcal/mol) electrostatic interaction with Asp 70 (Anderson et al., 1990). To investigate the strength of such ion pairs in general, it was necessary to introduce both a histidine and an aspartate as a double mutant. Three such double mutants, K60H/L13D, K83H/A112D, and S90H/Q122D, were constructed.

In designing the specific sites, the following criteria were followed: (a) The mutant sites should be either exposed or partially exposed to solvent. (b) The mutations should not interfere with existing hydrogen-bonding or salt bridge interactions seen in the X-ray structure. (c) Model building of the substituted side chains should permit a salt bridge to be constructed with good stereochemistry. Specifically, model building should allow a hydrogen bond (Baker & Hubbard, 1984) to be formed between the partners such that the side chains involved had rotamer angles within the limits specified by Ponder and Richards (1987). Table I lists the mutations selected, their presumptive salt bridge partners, and their solvent accessibilities. The locations of the mutations are shown in Figure 1. The putative salt bridge involving Glu 123 and Arg 125 is between the amino acids close together in the amino acid sequence, both within a short loop connecting two α-helices. In addition, Glu 123 could possibly interact with Arg 119, which would correspond to a salt bridge between residues at the *i* and *i*+4 positions in the α-helix that includes residues 115–123. Asn 144 is the second residue in the α-helix that includes residues 143–155. Therefore the putative interaction between Glu 144 and Lys 147 provides an example of a salt bridge between residues at the *i* and *i*+3 positions within an α-helix. The putative bridge between Lys 83 and

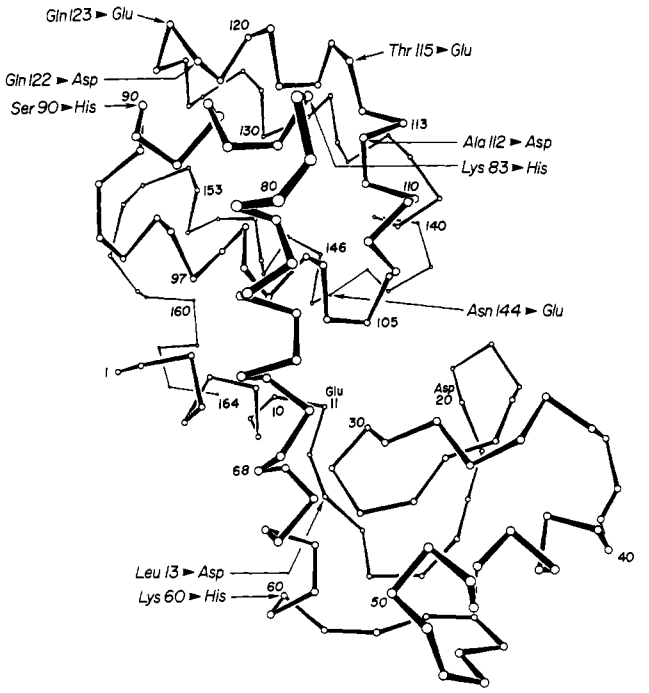

FIGURE 1: Backbone of T4 lysozyme showing the mutations used both to introduce putative salt bridges. The control mutations, used to delete the interacting partner, are not shown.

Glu 115 represents an interaction between two residues that are well separated (32 amino acids) in the linear sequence. Each of the putative His–Asp salt bridges also involves pairs of residues that are well spaced (32–47 amino acids) in the linear sequence. For disulfide bridges, the S–S link can be retained in the unfolded protein, and, for this reason, larger disulfide loops can contribute more to stability than smaller ones (Pace et al., 1988). In contrast, a salt bridge is presumably not retained in the unfolded protein, and the contribution of the salt bridge to stability is not expected to depend on the size of the polypeptide loop enclosed by the bridge.

To determine if the observed change in stability resulting from a given mutation was due to an interaction with its presumed partner, control mutants were made in which one of the charged groups was deleted. These control mutants were T115E/K83M, N144E/K147M, K60H, K83H, and S90H. Because Gln 123 is located between two arginines, it was not possible to design a simple control for the Gln 123 → Glu replacement and none was attempted.

Mutagenesis and Protein Purification. The mutants were created by site-directed mutagenesis following the uracil template method of Kunkel et al. (1987) as previously described (Dao-pin et al., 1991b). Mutants T115E and Q123E and their controls were created on the wild-type template, and the rest of the mutants were created on the pseudo-wild-type template, which has two auxiliary mutations C54T and C97A. The pseudo-wild-type template, denoted as WT*, eliminates the two cysteines present in wild-type lysozyme and facilitates the thermodynamic measurements (Pjura et al., 1990).

The mutant proteins were purified according to the normal procedure (Muchmore et al., 1989; Alber & Matthews, 1987; Poteete et al., 1991; Dao-pin et al., 1991). The cells were grown in 3 L of LB broth. Lysozyme expression was induced with IPTG. After harvest, mutant lysozyme proteins were isolated and purified on a 2.5 × 10 cm CM-Sepharose (Sigma CL-6B brand) ion-exchange column and then concentrated on a 1 × 5 cm SP Sephadex (Pharmacia C-50 brand) column. Each of the purified proteins was shown to be at least 95% pure when analyzed by HPLC.

Activity and Stability Measurements. Activities of the mutant lysozymes were assayed by the cell wall turbidity assay, in which the hydrolysis of cell walls was measured by the change in optical density at 350 μM (Tsugita et al., 1968). The protein concentration used in each assay was about 100 ng/mL. The assay buffer for T115E and Q123E was 10 mM sodium phosphate, pH 6.9. The remainder were measured in 50 mM Tris, pH 7.0.

The thermostabilities of the mutant lysozymes were measured over a range of pH by circular dichroism monitored reversible thermal denaturation (Elwell & Schellman, 1975), as described by Dao-pin et al. (1990). The protein concentration was about 20 μg/mL, and the buffer solutions were 10 mM HCl and 0.15 M KCl at pH 2; 10 mM potassium phosphate and 0.15 M KCl between pH 3 and 4 and at pH 6.5; and 10 mM acetate and 0.15 M KCl between pH 4 and 5.5.

Measurement of Histidine pK_a's. Titrations of the histidine mutants were carried out by proton NMR (Anderson et al., 1990). A sample of about 10 mg/mL of purified mutant protein bearing a histidine mutation was equilibrated with 10 mM KCl, 10 mM D_3PO_4, pH 2.5 buffer. The protein was then denatured at 55 °C for 30 min to allow the amide protons to exchange. The protein was refolded and equilibrated with 100 mM KCl, 10 mM deuterated phosphate buffer at a variety of pHs. The final sample protein concentration was 1 mg/mL. The chemical shift of the mutant histidine C-4 proton was recorded at 10 °C at different pHs with a 500-MHZ NMR spectrometer. The pH of each sample was measured after acquisition of the ^{1}H NMR spectrum, and the pK_a values were determined by fitting the pH-dependent chemical shifts with a titration curve (Anderson et al., 1990).

Structure Determination. Crystallization of the mutant proteins from approximately 2.0 M phosphate solutions at pH 6.7–7.0 was achieved under conditions similar to those for wild-type lysozyme (Weaver & Matthews, 1987; Brennan et al., 1988). For the variants that yielded crystals of suitable size for X-ray data collection, high-resolution X-ray diffraction data were collected with oscillation photography. The data were processed according to the method described by Weaver and Matthews (1987), and the mutant structures were refined with the TNT package (Tronrud et al., 1987). The typical procedure used to refine these and other mutant lysozymes is as described by Dao-pin et al. (1991a). Coordinates have been deposited in the Brookhaven Protein Data Bank.

RESULTS

Activities

The activities of the six primary mutant relative to the wild-type or pseudo-wild-type protein in which they were constructed are given in Table I. Much of the apparent difference in activity between wild-type lysozyme and the mutants T115E and Q123E is due to differences in the salt dependence of activity associated with these and other charge–change replacements [cf. Nicholson et al. (1988)]. The activity assay for T115E and Q123E was in 10 mM sodium phosphate, pH 6.9. Under such low-salt conditions, the activity is very salt dependent and increases by about a factor of 10 as the assay conditions are changed to 50 mM NaCl and 10 mM sodium phosphate, pH 6.9. As the concentration of NaCl is further increased, the activity decreases. At their respective maxima the activity of T115E is about 10% lower than that of wild-type lysozyme, while Q123E is about 20% higher (data not shown). In other words, the different variants all have similar overall activity profiles but can appear to have significant differences at low salt concentration because under such conditions activity is very salt dependent.

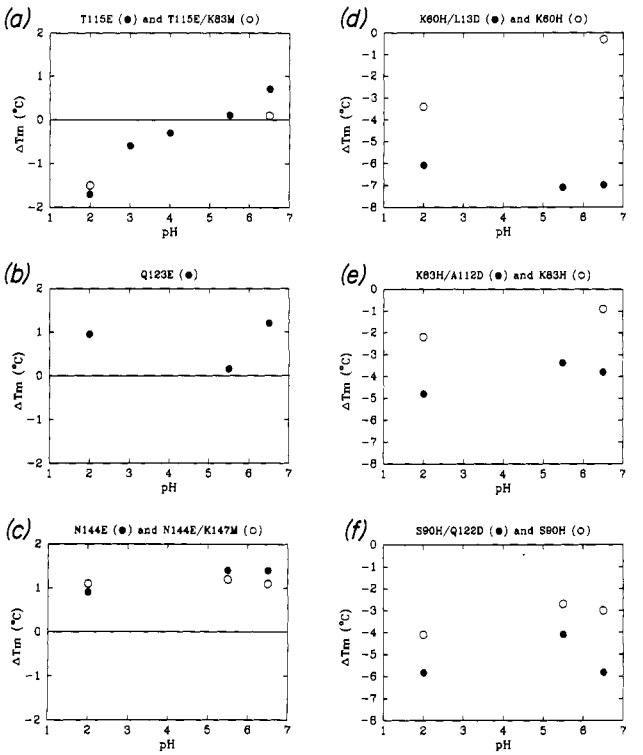

FIGURE 2: pH dependence of the difference between the melting temperatures of the mutant lysozymes and that of wild-type. The mutants T115E and Q123E and their controls were constructed in normal wild-type lysozyme, and their melting temperatures are shown relative to this parent. Mutants N144E, K60H/L13D, K83H/A112D, and S90H/Q122D and their controls were constructed in the pseudo-wild-type lysozyme C54T/C97A, and in these cases the melting temperatures are relative to this parent. (a) T115E (●) and control T115E/K83M (○). (b) Q123E (●) (in this case no control was attempted due to two nearby arginines with which Glu 123 might interact. (c) N144E (●) and control N144E/K147M (○). (d) K60H/L13D (●) and control K60H. (e) K83H/A112D (●) and control K83H (○). (f) S90H/Q122D (●) and control S90H (○).

Stabilities

The thermostabilities of the mutants were measured by circular dichroism monitored reversible thermal denaturation in the range from pH 2.0 to 6.5. The melting temperatures, enthalpies, and entropies of unfolding and the inferred changes in the free energy of unfolding of the six designed charge pair mutants and the five control mutants are listed in Table II. The differences in melting temperature are shown as a function of pH in Figure 2.

The electrostatic interaction between a pair of charged groups can in principle be estimated in two ways. First, it can be determined from the shifts in pK_a of the interacting groups in the folded relative to the unfolded protein (Cantor & Schimmel, 1980). Second, the energy of interaction can be obtained from changes in relative stability as a function of pH [e.g., Nicholson et al. (1988)].

For the mutants T115E, Q123E, and N144E, the electrostatic interaction can be estimated from the difference in stability at neutral pH, where the introduced glutamates and aspartates are charged, relative to the stability at lower pH, where they are not. As shown in Figure 2b,c, the stabilities of Q123E and N144E do not increase significantly relative to wild-type as the pH increases, suggesting that the electrostatic interaction of the introduced glutamate is weak. In the case of T115E (Figure 2a) there is a pronounced pH-dependent increase in stability, but about two-thirds of this increase is

Table II: Stabilities of Mutant Lysozymes[a]

primary mutants						control mutants					
pH	T_m (°C)	ΔH (kcal/mol)	ΔS (cal/deg·mol)	ΔT_m (°C)	$\Delta\Delta G$ (kcal/mol)	pH	T_m (°C)	ΔH (kcal/mol)	ΔS (cal/deg·mol)	ΔT_m (°C)	$\Delta\Delta G$ (kcal/mol)
		T115E						T115E/K83M			
2.0	38.7	84	269	−1.7	−0.5	2.0	38.9	86	275	−1.5	−0.5
3.0	52.0	117	359	−0.6	−0.2						
4.0	63.3	131	390	−0.3	−0.1						
5.5	66.8	126	370	0.1	0.04						
6.5	65.3	125	369	0.7	0.3	6.5	64.7	124	366	0.1	0.04
		Q123E									
2.0		82	259	1.0	0.3						
5.5		113	331	0.2	0.1						
6.5		132	390	1.2	0.4						
		N144E						N144E/K147M			
2.0	39.4	83	265	0.9	0.2	2.0	39.6	86	276	1.1	0.3
5.5	66.8	136	400	1.4	0.5	5.5	66.6	139	410	1.2	0.5
6.5	64.5	138	408	1.5	0.5	6.5	64.2	134	396	1.2	0.4
		K60H/L13D						K60H			
2.0	32.4	71	231	−6.1	−1.5	2.0	35.1	75	242	−3.4	−0.8
5.5	58.3	105	317	−7.1	−2.8						
6.5	55.9	82	249	−7.1	−2.8	6.5	62.6	115	341	−0.4	−0.1
		S90H/Q122D						S90H			
2.0	32.7	67	219	−5.8	−1.4	2.0	34.4	72	234	−4.1	−1.0
5.5	61.3	128	381	−4.1	−1.6	5.5	62.7	128	381	−2.7	−1.1
6.5	57.3	116	350	−5.7	−2.2	6.5	60.1	117	349	−2.9	−1.1
		K83H/A112D						K83H			
2.0	33.7	73	237	−4.8	−1.2	2.0	36.3	80	259	−2.2	−0.5
5.5	62.0	122	365	−3.4	−1.3						
6.5	59.1	119	356	−3.9	−1.5	6.5	62.0	122	364	−1.0	−0.4
		Wild-Type						WT* (C54T/C97A)			
2.0	40.4	99	315			2.0	28.5	77	246		
3.0	52.6	123	378								
4.0	63.6	143	422								
5.5	66.7	142	417			5.5	65.4	132	390		
6.5	64.6	125	371			6.5	63.0	131	391		

[a] T_m is the unfolding temperature of the mutant lysozyme and ΔT_m is the difference in T_m relative to the corresponding wild-type background (WT or WT*). The estimated uncertainty in ΔT_m is ± 0.5°C. ΔH and ΔS are the enthalpy and entropy of unfolding at T_m and have estimated uncertainties of ± 20%. $\Delta\Delta G$, the difference between the free energy of unfolding of the mutant and wild-type lysozyme is estimated from the relationship $\Delta\Delta G = \Delta S \cdot \Delta T_m$ (Becktel & Schellman, 1987), where ΔS is the entropy of unfolding of wild-type lysozyme at the corresponding pH. A positive value of $\Delta\Delta G$ indicates that the mutant is more stable than wild-type. The estimated uncertainty in $\Delta\Delta G$ is ± 0.15 kcal/mol. The measurements for T115E, T115E/K83M and the quoted values for wild-type lysozyme given in the table were all carried out as close in time as possible using the same solutions, the same cell, and identical experimental conditions. Similarly, the values for N144E, N144E/K147M, K60H/L13D, K60H, K83H/A112D, K83H, S90H/Q122D, S90H and WT* were also obtained as a set under identical conditions. All values are the average of at least three determinations. The values quoted for Q123E were measured twice at a different time and are quoted relative to a control WT* (data not included) which was measured in parallel. The practice of measuring each mutant in parallel with its own wild-type control ensures the most reliable determination of ΔT_m. For mutants similar in stability to wild-type, this, in turn, provides the most reliable estimate of $\Delta\Delta G$. For the same reason, and also because the experimental arrangement used in the unfolding experiments has evolved with time, the absolute values of T_m, ΔH and ΔS for wild-type and WT* given here do not necessarily correspond precisely with those quoted previously.

also observed for the control mutant T115E/K83M that lacks the engineered salt bridge. As will be discussed below, this non-salt-bridge component appears to be due to interaction of the glutamate with the amino terminal of an α-helix.

^{1}H NMR pK_a Measurements

The pK_a values of the substituted histidines in the three His–Asp mutants, K60H/L13D, K83H/A112D, and S90H/Q122D, together with the values in the control mutants K60H, K83H, S90H, as measured by ^{1}H NMR titration, are given in Figure 3. The titration curves are also shown.

The difference in pK_a values between the His–Asp double mutants and the single histidine control mutants should reflect the influence of the aspartates on the histidines in the double mutants. In the double mutants, the histidine pK_a is higher than in the corresponding single mutant, indicating, in each case, a favorable electrostatic interaction between the His–Asp charged pair. If this shift in pK_a is denoted ΔpK_a, then the corresponding increase in the electrostatic interaction energy of the histidine in the double mutant relative to the control structure ($\Delta\Delta G_E$) can be obtained (Cantor & Schimmel, 1980) as

$$\Delta\Delta G_E = 2.303RT(\Delta pK_a)$$

Thus, from the shifts in pK_a values shown in Figure 3, the His–Asp electrostatic interaction energies of the respective histidines in the K60H/L13D, K83H/A112D, and S90H/Q122D structures can be estimated as 0.8, 1.1, and 1.4 kcal/mol, respectively. These estimates assume that the pK_a values of the histidines in the unfolded double mutant and control proteins are the same. This is supported by the observation that the pK_a of His 31 is substantially perturbed in folded wild-type lysozyme but on unfolding assumes a value that is essentially identical with the pK_a of histidine in simple model compounds (Anderson et al., 1990).

Structures of Mutant Lysozymes

Of the six designed salt bridge mutants, T115E, Q123E, N144E, and K83H/A112D crystallized isomorphously with wild-type lysozyme in space group $P3_221$. High-resolution

Table III: Crystallographic Data Processing and Refinement Statistics

mutant	T115E	Q123E	N144E	K83H/A112D
		Data Collection		
cell dimensions				
a, *b* (Å)	61.0	61.1	61.1	60.6
c (Å)	96.6	96.7	96.9	96.9
resolution (Å)	1.85	1.80	1.85	1.75
unique reflections	13241	14378	12838	14683
completeness of data (%)	71	72	69	68
R_{merge} (%)	6.4	5.9	6.5	6.8
		Refinement Statistics		
resolution limits (Å)	6.0–1.85	6.0–1.8	6.0–1.85	6.0–1.75
no. of reflections used in the refinement	12768	13884	12138	14157
rms bond length dev (Å)	0.015	0.015	0.017	0.018
rms bond angle dev (deg)	2.34	2.17	2.30	2.37
rms dev from planarity (Å)	0.015	0.014	0.016	0.016
R factor (%)	15.1	15.6	15.1	15.7

X-ray crystallographic structures of these mutants were determined. Data collection and refinement statistics are given in Table III. Mutant K60H/L13D failed to crystallize and S90H/Q122D crystallized with a different space group, $P222_1$, with the cell dimensions a = 84.2 Å, b = 110.5 Å, and c = 138.8 Å.

Structure of T115E. The structure of mutant T115E was determined at 1.9-Å resolution and refined to a crystallographic *R* factor of 15.1%. The map showing the difference between the mutant and the wild-type structure is shown in Figure 4a. The large negative feature surrounding the wild-type Thr 115 side chain is due to the reduction in electron density at the γ-position. The large adjacent positive feature indicates the position of the longer Glu 115 side chain. The map is largely featureless other than in the vicinity of the mutation site. The refined T115E mutant structure superimposed on the wild-type structure in the vicinity of the mutation is shown in Figure 4b. Overall, the mutant structure is very similar to wild-type with a rms deviation between the respective backbone atoms of 0.11 Å. The side chain of Thr 115 in the wild-type structure is mainly exposed to solvent. The only hydrogen bond made by OG1 of Thr 115 is with the solvent molecule OH516 (distance 3.2 Å), shown in Figure 4b. The distance from OG1 of Thr 115 to the carbonyl oxygen of Phe 114 (Figure 4a) (3.6 Å) is long for a H-bond, and the geometry also is poor. The substituted side chain is also solvent exposed and appears to make hydrogen bonds with surface solvent only. The distance between OE2 of Glu 115 and the solvent molecule OH516 is 3.7 Å. There is no indication that Lys 83 moves toward the glutamate that is introduced at position 115 (Figure 4b). The closest approach between the carboxylate of Glu 115 and the ε-amino group of Lys 83 is 5.4 Å. The side chain of Glu 115 is found to be mobile with an average *B* value for atoms within the side chain of 69 Å^2. This can be compared with 34 Å^2, the average of the side-chain *B* values for the whole structure. The side chain of Lys 83 is relatively mobile in wild-type lysozyme, with an average thermal factor of 57 Å^2, and remains equally mobile (side-chain *B* of 66 Å^2) in T115E (Table IV).

Structure of Q123E. The structure of Q123E was refined at 1.8-Å resolution to a crystallographic residual of 15.6%. Overall, the mutant structure is very similar to the wild-type with a root-mean-square difference between main-chain atoms of 0.07 Å. This is indicated by the lack of features in the map showing the difference in electron density between the mutant and wild-type structures (Figure 5a). The overlay of the refined Q123E structure on wild-type is shown in Figure 5b. Both Arg 119 and Arg 125 are within 3–4 Å of the side chain of Glu 123 and remain very mobile, as in the wild-type structure. The averaged side-chain *B* values of Gln/Glu 123, Arg 119, and Arg 125 are 40.8, 62.0, and 54.7 Å^2 in the Q123E structure and are 40.6, 64.3, and 47.9 Å^2 in wild-type lysozyme. The geometry (Figure 5b) does not suggest that either of the arginines makes a strong hydrogen bond with Glu 123.

Table IV: Average Side-Chain Crystallographic Thermal Parameters of Residues Participating in Engineered Salt Bridges[a]

wild-type structure		mutant structures			
side chain	*B* (Å^2)	side chain	*B* (Å^2)	side chain	*B* (Å^2)
Lys 83	57	Lys 83	66	Glu 115	69
Arg 119	64	Arg 119	62	Glu 123	41
Arg 125	48	Arg 125	55		
Lys 147	43	Lys 147	42	Glu 144	39
Arg 148	16	Arg 148	17		

[a] The average thermal factor for all side chains in wild-type T4 lysozyme is 34 Å^2.

Structure of N144E. The structure of the mutant N144E was refined at 1.85-Å resolution to a crystallographic residual of 15.2%. The overall mutant structure is very similar to wild-type lysozyme with the root-mean-square difference between the two main-chain atoms of 0.11 Å. The map showing the difference between the mutant and wild-type structures is shown in Figure 6a. The whole map is relatively featureless aside from the mutation site. At this position, the mutant residue, Glu 144, appears to occupy two conformations, a major one with the side chain directed toward Arg 148 and a minor one with Glu 144 directed toward Lys 147. The two conformations of Glu 144 were refined with 60% and 40% occupancies, respectively, and are shown in Figure 6b,c. In the major conformation (Figure 6b), oxygen OE1 of Glu 144 makes a 3.0-Å hydrogen bond with a solvent molecules (OH287) that in turn makes a 2.9-Å hydrogen bond to NH_2 of Arg 148. The second oxygen (OE2) of Glu 144 is hydrogen bonded to another solvent molecule (OH194). In the alternative conformation of Glu 144, the oxygen OE2 makes a 2.8-Å hydrogen bond with NZ of Lys 147, and OE1 makes a 3.0-Å hydrogen bond with solvent molecule OH178. In contrast, Asn 144 in the wild-type structure makes only one 3.0-Å hydrogen bond, this being between OD1 and solvent molecule OH194. The averaged side-chain *B* values of residues 144, 147, and 148 are 38.8, 41.9, and 16.5 Å^2 in the mutant structure and 23.0, 42.5, and 15.7 Å^2 in the wild-type structure. In the difference map (Figure 6a), there is negative density at the position where a chloride ion is bound at the N-terminus of α-helix 143–153. A very similar feature was seen when Asn 144 was replaced with Asp (Nicholson et al., 1988). The *B* value of this chloride ion is 9.2 Å^2 in the wild-type structure

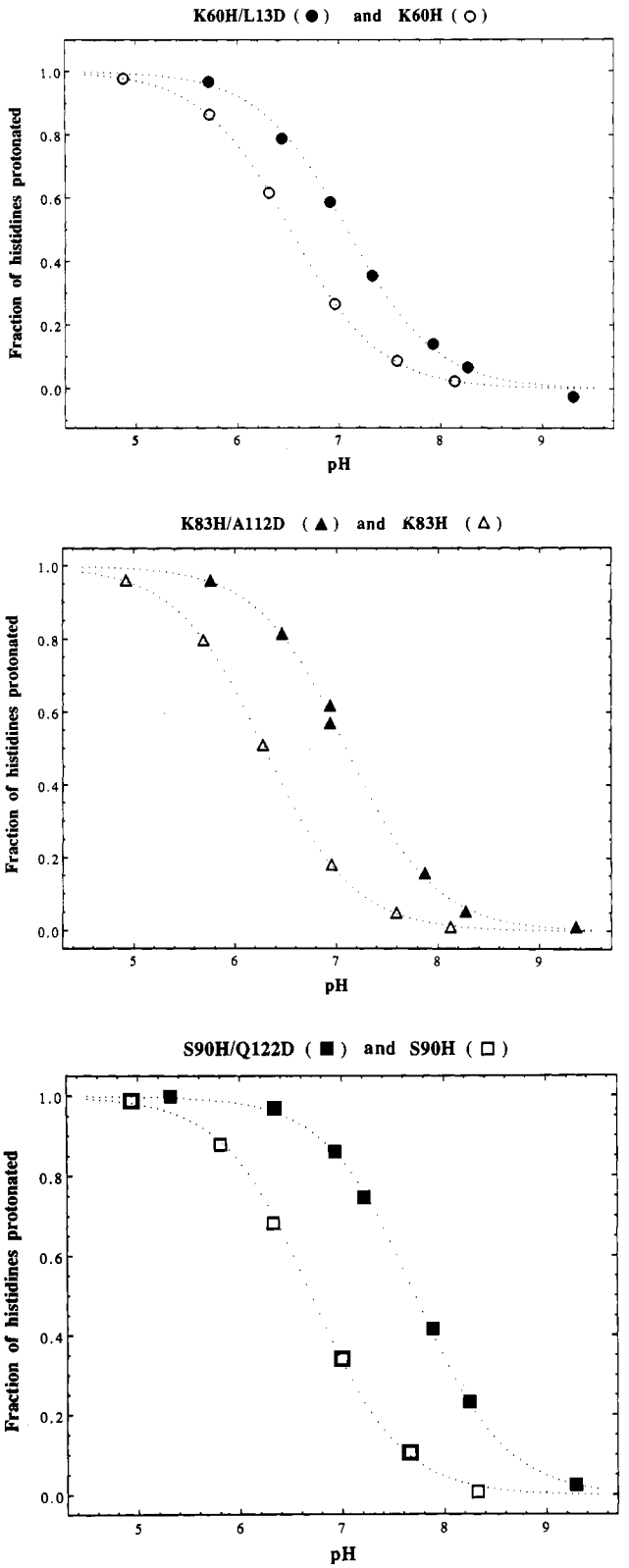

FIGURE 3: Titration of histidine-containing mutants determined by ^{1}H NMR. The dotted lines show the calculated titration curves for a single histidine with a pK_a as indicated. (a) K60H/L13D (●), pK_a = 7.1; K60H, pK_a = 6.5. (b) K83H/A112D (▲), pK_a = 7.1; K83H, pK_a = 6.3. (c) S90H/Q122D (■), pK_a = 7.7; S90H (□), pK_a = 6.7.

and 17.5 Å^2 in the mutant, suggesting that it may be replaced by water or it could become less well ordered and still remain bound.

Structure of K83H/A112D. The structure of the K83H/A112D double mutant was refined at 1.75-Å resolution to a 15.7% crystallographic R factor. The difference electron density map for this structure is shown in Figure 7a. There is a positive feature adjacent to CB of Ala 112 that is due to the substitution of Asp 112. As well, there are also several pairs of positive and negative features near residues 109 and 112 that indicate main-chain shifts due to the introduction of the two mutations. There is weak density for the introduced His 83 and Asp 112 side chains suggesting that they are relatively mobile. This is also indicated by the high thermal factors for the side-chain atoms in the refined structure, with values of 57 and 64 Å^2 for the averages of the respective side-chain atoms. Figure 7b shows the refined K83H/A112D mutant structure superimposed on the wild-type structure in the vicinity of the mutation sites. The largest structural difference between the mutant and wild-type is between residues 107 and 114, which form a distorted α-helix. As a result of the mutations this helix shifts away from His 83 by about 0.6 Å (Figure 8). The movement of residues 111 and 112 can also be seen in Figure 7b. In the mutant structure the side chain of Asp 112 is about 4 Å from His 83 with no hydrogen bond formed between them. Instead, both His 83 and Asp 112 in the mutant structure form weak hydrogen bonds with the side chain of Asn 81. The distance between the ND1 of His 83 and OD1 of Asn 81 is 3.5 Å, and the distance between the OD1 of Asp 112 and ND2 of Asn 81 is 3.4 Å. The overall root-mean-square difference between the mutant and wild-type main-chain atoms is 0.23 Å.

Discussion

Structures and Stabilities of the Mutant Lysozymes

Mutant T115E. The stability of the mutant T115E increases as the pH is increased from pH 2.0 to 6.5 (Figure 2a). This is exactly as anticipated if there were an electrostatic interaction involving Glu 115 because the glutamate would be expected to titrate within this pH range and be negatively charged above about pH 5. However, although the stability of the mutant T115E increases by about 0.8 kcal/mol, the control mutant T115E/K83M, in which the lysine is replaced by methionine, also shows an increase in stability of 0.54 kcal/mol within the same pH range (Table II). Thus the apparent energy of the Glu 115···Lys 83 electrostatic interaction is about 0.25 kcal/mol. In the mutant crystal structure (Figure 4b), Lys 83 shows no tendency to move toward Glu 115. The carboxylate of the introduced glutamate remains about 5 Å from the ϵ-amino group of Lys 83. This also does not suggest a strong interaction between Glu 115 and Lys 83. What, then, is the origin of the pH-dependent increase of stability seen in both T115E and T115E/K83M? The most likely explanation is an electrostatic interaction between Glu 115 and the effective positive charge at the amino terminus of α-helix 115–123 (Figure 4b). It has been shown previously that the introduction of aspartic acids at or close to the amino termini of α-helices can increase the thermostability of T4 lysozyme (Nicholson et al., 1988). In particular, the replacement of the adjacent residue, Asn 116, with Asp is such a stabilizing substitution. The Thr 115 → Glu replacement is at the beginning of the 115–123 helix and is also well placed to interact favorably with the α-helix dipole. It might be noted that even though residue 115 is at the beginning of the α-helix, Glu 115 in the mutant structure does not seem to act as a hydrogen-bonding "helix cap". The shortest distances between OE1 or OE2 of Glu 115 and the backbone amide nitrogens (N115 and N116) in the first turn of the α-helix are 5.9 and 4.5 Å, respectively. These are well beyond normal H-bonding distances. As can be seen in Figure 4b the backbone geometry

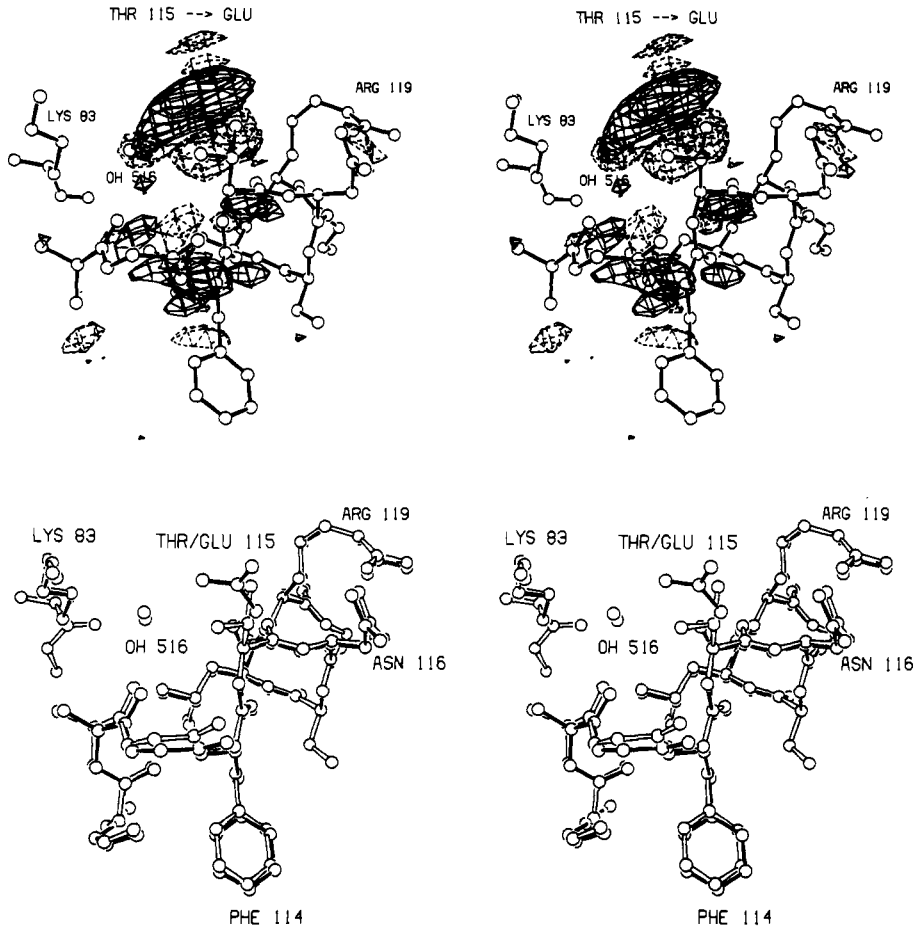

FIGURE 4: (Top, a) Map showing the difference in electron density between mutant T115E and wild-type lysozyme in the vicinity of the mutation. Amplitudes are the difference between the observed structure amplitudes for the mutant and wild-type lysozyme; phases were from the refined wild-type structure. Map contoured at $\pm 3\sigma$ where σ is the root-mean-square difference density throughout the unit cell. Positive contours are drawn solid; negative contours are drawn as broken lines. The most obvious features correspond to the loss of the γ-hydroxyl of the threonine (negative) and the introduction of the carboxylate of Glu 115 (positive). Note the absence of any positive or negative density near Lys 83, indicating that this residue does not move toward Glu 115. (Bottom, b) Superposition of the refined structure of T115E (open bonds) on that of wild-type lysozyme (solid bonds).

changes at residue 115 from α-helical toward 3_{10}, and this presumably prevents the side chain of Glu 115 from forming helix-cap H-bonds. This is consistent with the observation that favorable interaction with an α-helix dipole does not require hydrogen bonding between the substituted amino acid and the end of the α-helix (Nicholson et al., 1988).

Mutant Q123E. In the case of the mutant Q123E, the crystal structure shows that the carboxylate of Glu 123 is about 3 Å from the guanidinium group of Arg 125 and about 4 Å from that of Arg 119 (Figure 5b). No direct hydrogen bonding between these groups is apparent. Because of the possibility that the introduced glutamate at residue 123 could interact with either Arg 125 or Arg 119, or both, no control mutation was constructed. At maximum, the Gln → Glu replacement increases the stability of lysozyme by 0.4 kcal/mol (Table II). There is no evidence that the structure is significantly perturbed (Figure 5b). Because the increase in stability is essentially the same at pH 2.0 and 6.5 (Figure 2b), it does not suggest that the stabilization is due to an electrostatic effect.

Mutant N144E. In the mutant N144E, the contribution due to pH-dependent interactions, relative to the control mutant, again is small (about 0.2 kcal/mol; Table II, Figure 2c). The mutant and the control appear to be stabilized somewhat by hydrogen-bonding interactions that are pH independent. In the mutant structure (at pH 6.7) Glu 144 displays two conformations. In the major conformation the side chain forms a hydrogen bond to a solvent molecule OH287, which in turn hyrogen bonds to Arg 148. In the minor conformation, there is a 2.8-Å salt bridge with Lys 147. Because it is the minor conformation of Glu 144 that includes this salt bridge, it suggests that the electrostatic interaction is relatively weak. Previously it was shown that the replacement Asn 144 → Asp stabilizes T4 lysozyme by about 0.8 kcal/mol, the increase in stability being attributed to an electrostatic interaction of Asp 144 with the dipole of α-helix 144–153 (Nicholson et al., 1988). Asp 144 was observed to extend into solvent and not to form H-bonds with the backbone amides in the first turn of the α-helix. Glu 144 also extends into solvent in both its major and minor configuration and in neither case makes H-bonds with the backbone amides in the first turn of the helix (Figure 6b,c). Because Glu 144 appears to occupy two conformations, one closer to Lys 147 and the other closer to the end of α-helix 144–153, and also because the observed stabilization is largely pH independent (Figure 2c), it is difficult to rationalize the underlying causes.

Mutant K83H/A112D. The K83H/A112D double mutant, which was designed to introduce a His···Asp salt bridge, has much larger changes in three-dimensional structure than was observed for any of the previously described single mutants. The overall root-mean-square difference between the main-chain atoms in K83H/A112D and wild-type lysozyme is 0.23 Å. This is twice as large as observed for T115E, Q123E, or N144E. In the double mutant, the introduced changes cause backbone atoms within the α-helix from residue 107 to 114

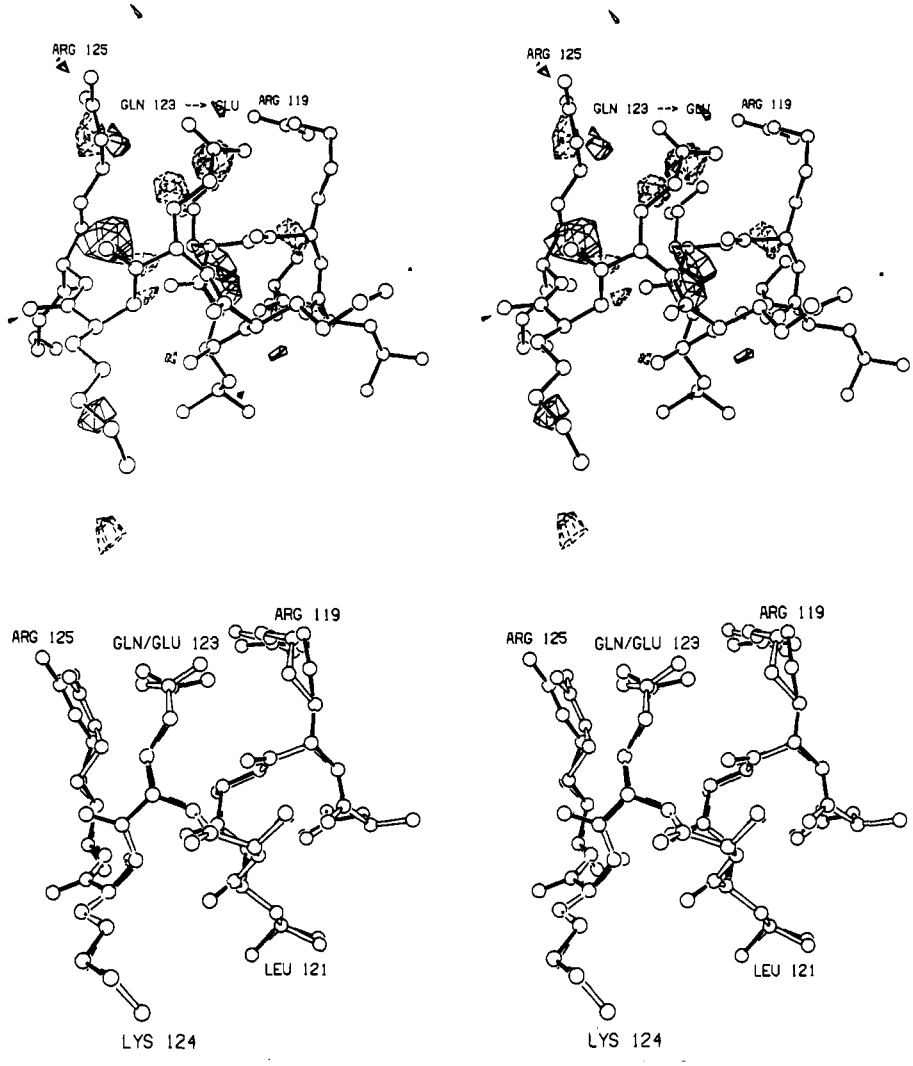

FIGURE 5: (Top, a) Map showing the difference in electron density between Q123E and wild-type lysozyme. All conventions are as in Figure 4a. (Bottom, b) Superposition of the structure of Q123E (open bonds) on that of wild-type lysozyme (solid bonds).

to move between 0.4 and 0.8 Å (Figure 8). The initial model building suggested that it would be possible for His 83 to make a hydrogen bond to Asp 112. In the observed crystal structure, however, the imidazole of His 83 is rotated relative to the orientation envisaged in the model-building experiment and makes a different H-bond, namely to the δ-oxygen of Asn 81 (Figure 7b).

Although the charge–charge interaction between His 83 and Asp 112 gives rise to 1.1 kcal/mol of favorable stabilization energy as measured by the shift in pK_a of His 83 (Figure 3b), the amino acid replacements also introduce strain, reflected in the alteration in the local main-chain structure, that results in an overall destabilization of the mutant lysozyme structure. Consistent with this argument, the control single mutant, K83H, has stability between that of the K83H/A112D and that of wild-type (Figure 2e). This suggests that the Lys 83 → His replacement destabilizes the folded structure, and the subsequent replacement Ala 112 → Asp causes further destabilization that is not compensated by the interaction between His 83 and Asp 112.

Mutants K60H/L13D and S90H/Q122D. Both K60H/L13D and S90H/Q122D substantially destabilize T4 lysozyme (Figure 2d,f). No structures are available for these variants, although in each case one of the mutation sites is relatively inaccessible to solvent (Table I), suggesting that replacements at such positions could cause structural perturbations or might destabilize the structure because of partial burial of the introduced charge. Again, although the introduced histidines have shifted pK_a's (Figure 3a,c), indicating that they participate in favorable electrostatic interactions in the mutant structures, these contributions to stability are overwhelmed by the apparent strain introduced into the double mutant structures. In terms of designing stabilizing salt bridges, the introduction of the His···Asp pair has the double disadvantage that two existing amino acids must be removed without the loss of favorable interactions and that neither the Asp nor the His should introduce strain. For these reasons, it may be difficult to find fully satisfactory sites.

Salt Bridges within α-Helices

Recently there has been considerable discussion concerning the stabilization of α-helices by salt bridge interactions between charged groups in successive turns of the helix (Marqusee & Baldwin, 1987; Marqusee et al., 1989; Sundaralingam et al., 1987; Lyu et al., 1989, 1990; Serrano et al., 1990; Perutz & Fermi, 1988; Lyu et al., 1991). Three of the mutations described here could, at least in principle, introduce putative salt bridges that are of this type.

The replacement of Thr 115 with Glu was designed to introduce a salt bridge with Lys 83, but it also happens that residues 115–123 form an α-helix and include an arginine at position 119 (Figure 4b). An interaction between Arg 119 and Glu 115 would be an example of an $i\cdots i+4$ charged pair. The mutant T115E is 0.8 kcal/mol more stable at pH 6.5 than

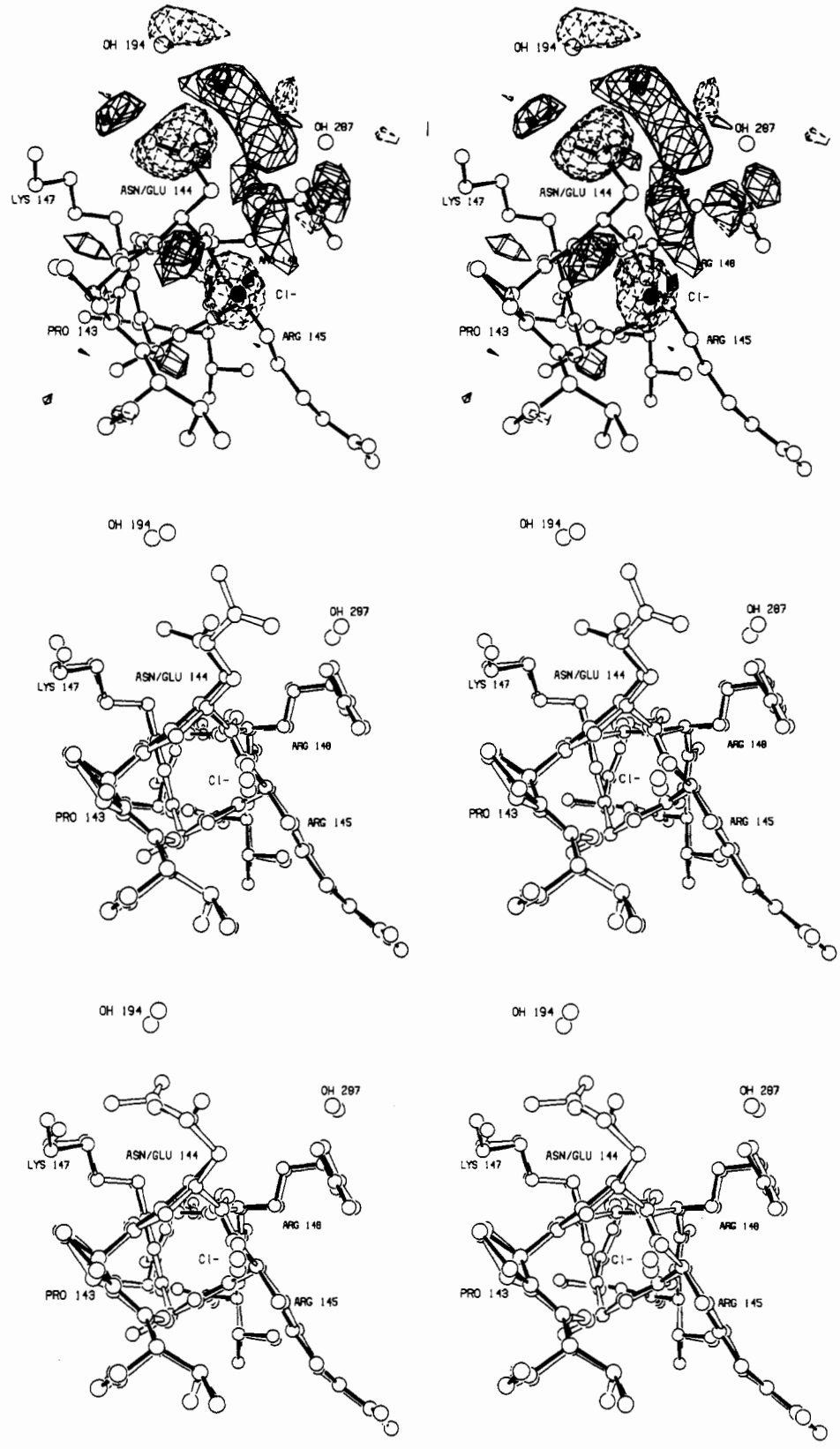

FIGURE 6: (Top, a) Difference in density between N144E and wild-type lysozyme. All conventions are as in Figure 4a. The black circle shows a chloride ion that is bound at this site in the crystal structure of wild-type lysozyme and is displaced in the mutant as it also is in the "helix capping" replacement N144D (Nicholson et al., 1988). (Middle, b) Superposition of N144E (open bonds) on wild-type lysozyme (solid bonds) showing the predominant conformation adopted by Glu 144. Solvent molecules seen in the wild-type structure are shown as dark circles. Those seen in the mutant structure are shown as light circles. (Bottom, c) Superposition of N144E (open bonds) on wild-type lysozyme (solid bonds) showing the second conformation adopted by Glu 144.

at pH 2.0, indicative of a favorable electrostatic interaction. In the control mutant, when Lys 83 is replaced by methionine, the increase in stability at pH 6.5 relative to pH 2.0 is reduced by 0.26 kcal/mol (Table II), which we take as a measure of the contribution from the Lys 83···Glu 115 salt bridge. The control mutant T115E/K83M, which lacks the Lys 83···Glu

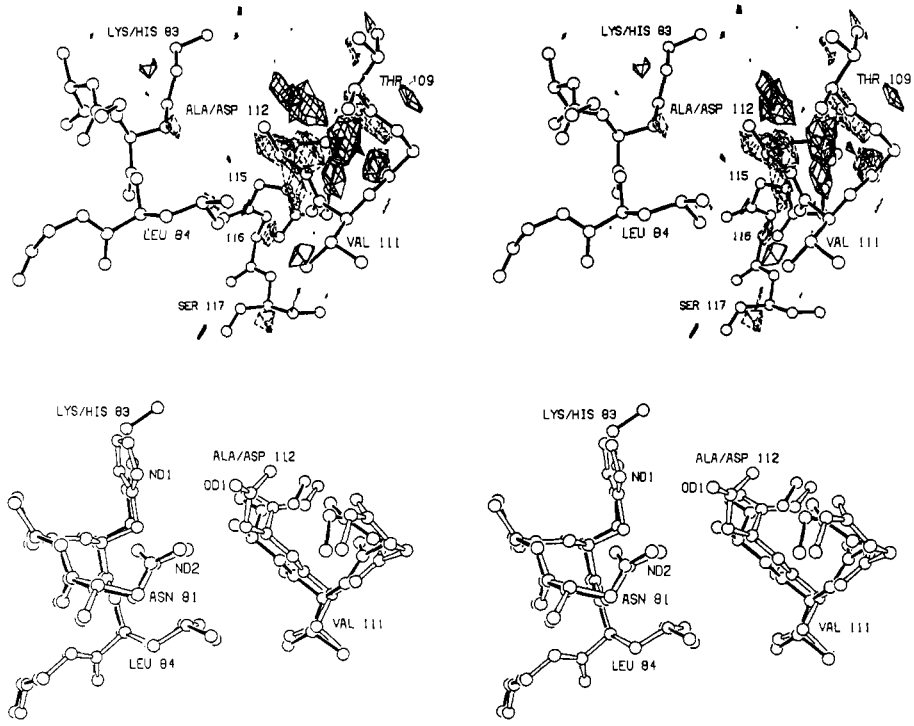

FIGURE 7: (Top, a) Map showing the difference in electron density between the mutant K83H/A112D and wild-type lysozyme. All conventions as are in Figure 4a. (Bottom, b) Superposition of the structure of K83H/A112D (open bonds) on that of wild-type lysozyme (solid bonds).

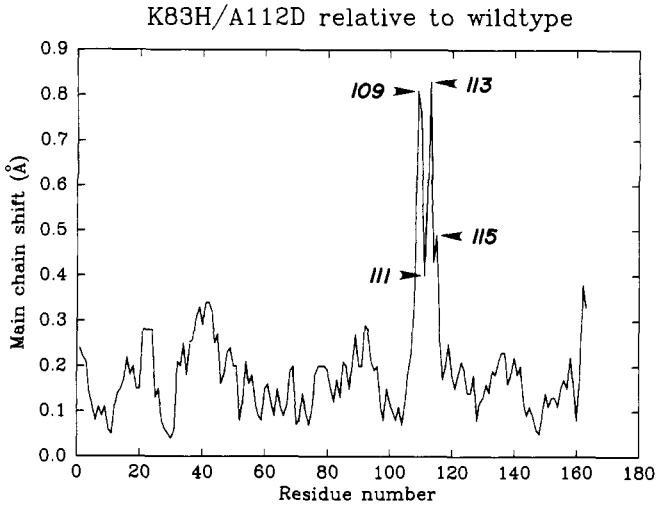

FIGURE 8: "Shift plot" showing the displacement between the backbone atoms of K83H/A112D lysozyme and that of wild-type. For each residue the shift shown is the average of the four backbone atoms C, O, CA, and N. Prior to making the plot, the respective structures were superimposed so as to minimize the root-mean-square displacement between all atoms. The relative movement of the α-helix that includes residues 107–114 is apparent.

115 salt bridge, still displays an increase in stability of 0.54 kcal/mol as the pH is increased from 2.0 to 6.5 (Table II). The pH dependence of this increase in stability suggests that it is due to some residual electrostatic interaction involving Glu 115. The most likely candidate is an interaction between Glu 115 and the "α-helix dipole" at the amino terminus of α-helix 115–123. An interaction energy of 0.54 kcal/mol would be very much in line with the stabilization observed for acidic groups introduced close to the amino termini of other α-helices of T4 lysozyme (Nicholson et al., 1991). Although it seems unlikely, we cannot, however, rule out an electrostatic interaction between Glu 115 and Arg 119 in the next turn of the α-helix. In the crystal structure of T115E (Figure 4b) there is no evidence of a direct interaction between Glu 115 and Arg 119. Rather, Glu 115 appears to hydrogen bond to Asn 116, which in turn hydrogen bonds to Arg 119. Asn 116, an intervening residue in the α-helix between Glu 115 and Arg 119, therefore appears to ameliorate possible direct interaction between them. This example illustrates clearly how the interactions between residues in an α-helix depend not only on their identity and spacing but also on the nature of other amino acids within the helix.

The replacement of Gln 123 with Glu introduces possible electrostatic interactions between the glutamate and both Arg 125 and Arg 119. The Arg 119···Glu 123 interaction is between residues i and i+4 in the α-helix 115–123 (Figure 5b). The apparent electrostatic contribution to stability resulting from the Gln 123 → Glu replacement is only 0.1 kcal/mol (Table II). This suggests that both the Glu 123···Arg 119 interaction and the Glu 123···Arg 125 interaction are very weak (although some type of offsetting interactions between these groups cannot be excluded). Because of possible multiple interactions, no control mutant was made in this case, although it might be noted that the primary mutation Gln 123 → Glu is very conservative, so that a control might not be so important in this case.

The replacement of Asn 144 with Glu was designed to introduce a salt bridge with Lys 147. Glu 144 is the second residue and Lys 147 the fourth residue of α-helix 143–155, so that the salt bridge is between residues i and i+3 (Figure 6b,c). Relative to the control mutant in which Lys 147 is replaced with methionine, the electrostatic contribution to stability from the Glu 144···Lys 147 salt bridge is 0.2 kcal/mol (Table II). In the N144E structure, the side chain of Glu 144

displays two alternative conformations, one directed toward Lys 147 (Figure 6c), indicative of a favorable interaction, but Glu 144 also populates a second conformation (Figure 6b), indicating that its interaction with Lys 147 is not a dominant one.

Thus, so far as salt bridge interactions within α-helices are concerned, the simplest interpretation of the data is that the $i\cdots i+3$ interaction between Glu 144 and Lys 147 contributes 0.2 kcal/mol to the stability of the helix, the contribution from the $i\cdots i+4$ interaction between Arg 119 and Glu 123 is essentially zero (not more than 0.1 kcal/mol), and the contribution from the $i\cdots i+4$ interaction between Glu 115 and Arg 119 is also small. This might be regarded as surprising since it has been argued that interactions of the form $i\cdots i+4$ tend to be more beneficial than $i\cdots i+3$ interactions (Maxfield & Scheraga, 1975; Marqusee & Baldwin, 1987; Marqusee et al., 1989; P. C. Lyu, P. J. Gans, and N. R. Kallenbach, personal communication). Inspection of the relevant crystal structures, however, suggests that the observed results are not surprising. In general terms, it is to be expected that the strength of interaction between charged residues in successive turns of an α-helix will depend on the nature of the residues involved, the number of intervening amino acids, and the details of the geometry of interaction [cf. Perutz and Fermi (1988) and Merutka and Stellwagen (1991)]. The stereochemistry of an Arg···Glu ion pair, for example, is not the same as Glu···Arg. For the reasons discussed in the next section, the energy of interaction between two charged residues, either within an α-helix or in general, that are mobile and fully solvent exposed is likely to be weak (not more than about 0.25 kcal/mol). If, however, the charged partners tend to be held in the appropriate alignment by interactions with other residues in the vicinity (in particular by the influence of other residues within the α-helix), then a stronger or weaker salt bridge interaction could occur. Charged residues close to the ends of α-helices are likely to interact with the α-helix dipole and so need to be considered as special cases.

The Entropic Cost of Forming a Rigid Salt Bridge

The formation of a salt bridge requires that two groups of opposite charge be held within hydrogen-bonding distance of each other. The results shown here suggest that charged groups introduced on the surface of a protein do not form such well-defined salt bridges, even though they have the opportunity to do so. Also, the introduced charged partners are observed to have only a small effect on protein stability, suggesting that the energy of interaction is weak.

Formation of a structurally defined salt bridge between mobile side chains has an entropic cost. Consider, for example, the consequences of restricting rotation about the C^{α}–C^{β} bond of a single side chain. If the number of conformations accessible to χ_1 when no salt bridge is present is denoted $\gamma_{\chi_{1,nsb}}$, and the formation of the salt bridge reduces the number of conformations to $\gamma_{\chi_{1,sb}}$, then the entropic free energy cost associated with this restriction in degrees of freedom (Nemethy et al., 1966) is

$$\Delta\Delta G = RT \ln (\gamma_{\chi_{1,nsb}}/\gamma_{\chi_{1,sb}})$$

If we assume that the formation of a salt bridge halves the number of available conformations, the corresponding entropy cost would be about 0.4 kcal/mol. Therefore, to localize two flexible side chains, each with two degrees of rotational freedom (e.g., χ_1 and χ_2), might require on the order of 1.6 kcal/mol. Let us also suppose that, as a result of a spatially defined salt bridge, the average separation between the oppositely charged groups is reduced from 5 to 3 Å. If the groups are highly solvated and the dielectric constant presumed to be 80, the same as water, then the calculated electrostatic energy will increase from 0.8 to 1.4 kcal/mol. The increase of 0.6 kcal/mol is comparable with the estimated entropy cost of localizing a single side chain but is substantially less than the energy required for two partners. The estimated values for both the electrostatic interaction and the entropy cost are crude approximations, but they are consistent with the notion that one will tend to offset the other. It is also observed that solvent-exposed charged groups on the surfaces of proteins often retain high mobility even when there are oppositely charged groups nearby with which they might interact. The structure of T4 lysozyme has recently been determined at high, medium, and low salt concentrations (Bell et al., 1991). Even in the presence of low salt, where electrostatic interactions would be expected to be stronger, there was no noticeable tendency of the charged groups on the surface of the protein to form better ordered ion pairs.

It has to be remembered that protein stability as quoted herein refers to the difference between the stability of the folded and the unfolded polypeptide chains. A mutation could change stability by an effect on either the folded or the unfolded species, or on both. The effects of the mutations described here can be easily rationalized in terms of the observed crystal structures, i.e., the putative salt bridge partners remain mobile and show no indication of significant electrostatic attraction, consistent with their small effect on protein stability. For this reason, one has no need to invoke the unfolded state. Nevertheless it cannot be ignored. One might argue, for example, that the engineered salt bridge partners do interact strongly in the folded protein and the salt bridges are retained in the unfolded state, so that they have little or no net effect on stability. On general grounds, we think this very unlikely since there is no indication that the charge partners make well-defined interactions even when they are engineered to be close together on the surface of the protein, let alone in the unfolded state. More important, however, if a specific salt-bridge were retained in the unfolded state, it would restrict the conformational freedom of the polypeptide backbone between the charged partners, decreasing the entropy of the unfolded state and increasing the energy of the folded relative to the unfolded form. This is not observed.

Conclusions

In summary, single mutations that were designed to introduce salt bridges on the surface of T4 lysozyme increased the stability of the protein by 0.0–0.5 kcal/mol. Control mutations, however, indicated that the contribution to stability from the engineered salt bridge was only about 0.1–0.25 kcal/mol. Attempts to introduce His···Asp salt bridges by pairs of amino acid replacements substantially destabilized the protein, presumably because of conformational strain introduced into the protein structure and loss of favorable interactions on removal of the wild-type side chains.

Results from other laboratories also indicate that engineered salt bridges on the surface of proteins contribute little to stability. Erwin et al. (1990) engineered ten salt bridges in subtilisin BPN′ and found that only one increased the melting temperature of the protein, the increase in this instance being 1.6 °C. Akke and Forsen (1990) engineered three salt bridges in calbindin and found that they increased stability by 0.1–0.7 kcal/mol. Similar results were reported by Horovitz et al. (1990), Serrano et al. (1990), and Pace et al. (1990).

Pairs of oppositely charged residues on the surface of a protein that have the freedom to adopt different conformations

do not tend to come together to form structurally localized salt bridges. Rather, such residues tend to remain mobile, interact weakly if at all, and do not contribute significantly to protein stability. The entropic cost of localizing a pair of mobile solvent-exposed charged groups on the surface of the protein largely offsets the interaction energy expected from the formation of a defined salt bridge. There are examples of strong salt bridges in proteins, but such examples require that supplemental interactions, in addition to the salt bridge itself, contribute part of the requisite driving energy to hold the interacting partners in the correct rigid alignment. Horovitz et al. (1990) have reported that multiple salt bridges in barnase have a cooperative effect such that the stabilization from multiple salt bridging is energetically more favorable than the sum of the constituent single bridges. This behavior can now be rationalized by noting that the entropy cost of localizing a charged residue in a single salt bridge comes from the energy of the bridge. In multiple salt bridging, however, the entropy cost is shared among the different interactions, resulting in a net increase in stability.

Acknowledgments

We thank Joan Wozniak for excellent technical assistance. We also thank Dr. Walt Baase for his advice and Dr. J. A. Schellman for providing the facilities for the thermodynamic analysis of the mutant lysozymes. We are most grateful to Eric Anderson for carrying out the histidine NMR titrations and Dr. F. W. Dahlquist for providing the NMR facilities. We thank Dr. N. Kallenbach for providing manuscripts in advance of publication.

References

Akke, M., & Forsen, S. (1990) *Proteins: Struct., Funct., Genet. 8*, 23–29.

Alber, T., & Matthews, B. W. (1987) *Methods Enzymol. 154*, 511–533.

Anderson, D. E., Becktel, W. J., & Dahlquist, F. W. (1990) *Biochemistry 29*, 2403–2408.

Baker, E. N., & Hubbard, R. E. (1984) *Prog. Biophys. Mol. Biol. 44*, 97–179.

Barlow, D. J., & Thornton, J. M. (1983) *J. Mol. Biol. 168*, 867–885.

Becktel, W. J., & Schellman, J. A. (1987) *Biopolymers 26*, 1859–1877.

Bell, J. A., Wilson, K. P., Zhang, X.-J., Faber, H. R., Nicholson, H., & Matthews, B. W. (1991) *Proteins: Struct., Funct., Genet. 10*, 10–21.

Brennan, R. G., Wozniak, J. A., Faber, R. H., & Matthews, B. W. (1988) *J. Cryst. Growth 90*, 160–167.

Brown, L. R., De Marco, A., Richarz, R., Wagner, G., & Wuthrich, K. (1978) *Eur. J. Biochem. 88*, 87–95.

Cantor, C. R., & Schimmel, P. R. (1980) *Biophysical Chemistry, Part 1. The Conformation of Biological Macromolecules*, pp 44–45, W. H. Freeman, San Francisco, CA.

Dao-pin, S., Baase, W. A., & Matthews, B. W. (1990) *Proteins: Struct., Funct., Genet. 7*, 198–204.

Dao-pin, S., Alber, T., Baase, W. A., Wozniak, J. A., & Matthews, B. W. (1991a) *J. Mol. Biol.* (in press).

Dao-pin, S., Söderlind, E., Baase, W. A., Wozniak, J. A., Sauer, U., & Matthews, B. W. (1991b) *J. Mol. Biol.* (in press).

Elwell, M. & Schellman, J. A. (1975) *Biochim. Biophys. Acta 386*, 309–323.

Erwin, C. R., Barnett, B. L., Oliver, J. D., & Sullivan, J. F. (1990) *Prot. Eng. 4*, 87–97.

Fersht, A. R. (1972) *J. Mol. Biol. 64*, 497–509.

Horovitz, A., Serrano, L., Avron, B., Bycroft, M., & Fersht, A. R. (1990) *J. Mol. Biol. 216*, 1031–1044.

Kunkel, T. A., Roberts, J. D., & Zakour, R. A. (1987) *Methods Enzymol. 154*, 367–382.

Lee, B., & Richards, F. M. (1971) *J. Mol. Biol. 55*, 379–400.

Lyu, P. C., Marky, L. A., & Kallenbach, N. R. (1989) *J. Am. Chem. Soc. 111*, 2733–2734.

Lyu, P. C., Gans, P. J., & Kallenbach, N. R. (1991) *Nature* (submitted).

Marqusee, S., & Baldwin, R. L. (1987) *Proc. Natl. Acad. Sci. U.S.A. 84*, 8898–8902.

Marqusee, S., Robbins, V. H., & Baldwin, R. L. (1989) *Proc. Natl. Acad. Sci. U.S.A. 86*, 5286–5290.

Maxfield, F. R., & Scheraga, H. A. (1975) *Macromolecules 8*, 491–493.

Merutka, G., & Stellwagen, E. (1991) *Biochemistry 30*, 1591–1594.

Muchmore, D. C., McIntosh, L. P., Russell, C. B., Anderson, D. E., & Dahlquist, F. W. (1989) *Methods Enzymol. 177*, 44–73.

Nemethy, G., Leach, S. J., & Scheraga, H. A. (1966) *J. Phys. Chem. 70*, 998–1004.

Nicholson, H., Becktel, W., & Matthews, B. W. (1988) *Nature 336*, 651–656.

Nicholson, H., Anderson, D. E., Dao-pin, S., & Matthews, B. W. (1991) *Biochemistry* (submitted).

Pace, C. N., Grimsley, G. R., Thomson, J. A., & Barnett, B. J. (1988) *J. Biol. Chem. 263*, 11820–11825.

Pace, C. N., Laurents, D. V., & Thornton, J. A. (1990) *Biochemistry 29*, 2564–2572.

Perutz, M. F. (1978) *Science 201*, 1187–1191.

Perutz, M. F., & Fermi, G. (1988) *Proteins: Struct., Funct., Genet. 4*, 294–295.

Pjura, P. E., Matsumura, M., Wozniak, J. A., & Matthews, B. W. (1990) *Biochemistry 29*, 2592–2598.

Ponder, J. W., & Richards, F. M. (1987) *J. Mol. Biol. 193*, 775–791.

Poteete, A. R., Dao-pin, S., Nicholson, H., & Matthews, B. W. (1991) *Biochemistry 30*, 1425–1432.

Serrano, L., Horovitz, A., Avron, B., Bycroft, M., & Fersht, A. R. (1990) *Biochemistry 29*, 9343–9352.

Sundaralingam, M., Sekharudu, Y. C., Yathindra, N., & Ravichandran, V. (1987) *Proteins: Struct., Funct., Genet. 2*, 64–71.

Tronrud, D. E., Ten Eyck, L. F., & Matthews, B. W. (1987) *Acta Crystallogr. A43*, 487–503.

Tsugita, A., Inouye, M., Terzaghi, E., & Streisinger, G. (1968) *J. Biol. Chem. 243*, 392–397.

Wada, A., & Nakamura, H. (1981) *Nature 293*, 757–758.

Weaver, L. H., & Matthews, B. W. (1987) *J. Mol. Biol. 193*, 189–199.